

# Molecular stress function theory and analysis of branching structure in industrial polyolefins

Saeid Kheirandish · Manfred Stadlbauer

Rheological Analysis of Polymers/Special Chapter  
© Akadémiai Kiadó, Budapest, Hungary 2009

**Abstract** Despite substantial progress in analytical techniques for polymer characterization, a realistic picture of branching structure in industrial polymers still remains at large. Using a number of assumptions, structure-based constitutive models can distinguish between linear and branched structures in a qualitative sense. More detail on branching architecture, such as the number and length of side chains, the sequence in which they exist on the backbone and their contribution to polymer chain relaxation is more or less unknown. In the current study, elongational behavior of four commercial polyolefins is compared using the predictions of the MSF (molecular stress function) theory. The results will then be used to analyze the branching in a group of strain-hardening polypropylenes synthesized using single site catalyst.

**Keywords** Branched polyolefins · Constitutive equations · Elongational rheology · Molecular stress function theory

## Introduction

The polyolefin market is becoming increasingly demanding in terms of material properties. As polymers are being integrated further into various new industrial fields, there is a need to have an accurate picture of the material structure that is as specific as possible. Experimental rheology, on its

own part, has proven to produce very precise and consistent information in terms of structure–property relationships. Rheology has the unique feature that it can deal with single polymer molecules, and is capable of predicting the material behavior in processing operations which mostly include deformations with high degrees of complexity. Elongational behavior of polymers has a significant effect on material behavior in processing [1] and is very sensitive to polymer structure [2]. Industrial polyolefins are mostly provided in a variety of multi-modal, partially miscible blends to improve their processing properties [3–6]. In this respect, LCB (long chain branched) polymers often comprise the part that is added to improve processing by imparting stability. Strain-hardening is especially critical in applications where the melt is exposed to large elongational deformations such as foam expansion [7–9], extrusion coating [10, 11], blown film extrusion [12], and multi-layer film production [13].

However, industrial polyolefin systems are rheologically complex [4] and elongational rheology is normally the most reliable method to characterize their degree of branching. In order to interpret the rheological data and obtain a better understanding of material behavior, numerous theoretical methods have been established. The major challenge in the case of industrial polymers is to obtain a theoretical method which is (a) capable of predicting rheological behavior in uniaxial, planar, biaxial, and shear deformations, (b) uses a minimum number of assumed parameters, and (c) covers a wide range of structures. In this respect, the majority of constitutive models are modified versions of the tube theory of Doi and Edwards [14, 15]. The tube in Doi and Edwards (DE) model is a network of constraints caused by neighboring chains. The main two mechanisms affecting relaxation are distinguished based on their time scales  $\tau_R$  and  $\tau_d$ .  $\tau_R$  corresponds to chain retraction along the tube contour in

---

Dedicated to Professor Manfred H. Wagner on the occasion of his 60th birthday

---

S. Kheirandish (✉) · M. Stadlbauer  
Borealis Polyolefine GmbH, St. Peter Str. 25, 4021 Linz, Austria  
e-mail: saeid.kheirandish@borealisgroup.com

a fast process and is proportional to the square of the molar mass, and  $\tau_d$  corresponds to chain diffusion by reptation out of the tube (and subsequent disengagement) and it is proportional to the third power of the molar mass. However, it is known that the original scaling law is compromised as soon as the system becomes polydisperse [16, 17] and is rendered useless when branching is present in any form in the system [18].

**Molecular stress function theory**

In the case of non-linear deformations the DE theory assumes the stress to be produced by changes in the orientation of the chain and can be calculated using an integral constitutive equation of the form [15]:

$$\sigma = -p\mathbf{I} + \int_{-\infty}^t m(t-t') \mathbf{S}_{DE}^{IA}(t,t') dt' \tag{1}$$

Here,  $\mathbf{S}_{DE}^{IA}$  denotes the strain measure of the Doi-Ewards (DE) model with the independent alignment assumption and is given by:

$$\mathbf{S}_{DE}^{IA} = \frac{15}{4} \langle \frac{\mathbf{u}'\mathbf{u}'}{u'^2} \rangle = \frac{15}{4} \mathbf{S} \tag{2}$$

$u'$  denotes the deformed unit vector  $\mathbf{u}$  and  $\langle \dots \rangle$  is an integral over an isotropic distribution of unit vectors before deformation,

$$\langle \dots \rangle = \frac{1}{4\pi} \int \dots d\Omega \tag{3}$$

and  $m(t-t')$  is the memory function and can be calculated using the linear relaxation spectra:

$$m(t-t') = \sum_i \frac{g_i}{\tau_i} e^{-\frac{t-t'}{\tau_i}} \tag{4}$$

$g_i$  and  $\tau_i$  can be calculated using the data from oscillatory shear measurements.

The tube theory in this form gives incorrect predictions for the uniaxial elongational deformation. The reason for this discrepancy is shown schematically in Fig. 1. Upon inception of stress, the unit vector  $\mathbf{u}$  takes the intermediate value  $\mathbf{u}'$  and eventually becomes saturated and is equal to the normalized unit vector  $\mathbf{u}'/u'$ . This assumption leads to an early plateau of elongational viscosities which is contrary to experimental results for strain-hardening melts. Experimental evidence suggests that at deformation rates larger than the reciprocal characteristic relaxation time,  $\tau_R$ , chains are stretched and orientation alone cannot be accounted for the evolution of stress. The concept of chain stretch, also first mentioned by Doi and Edwrad [15] and

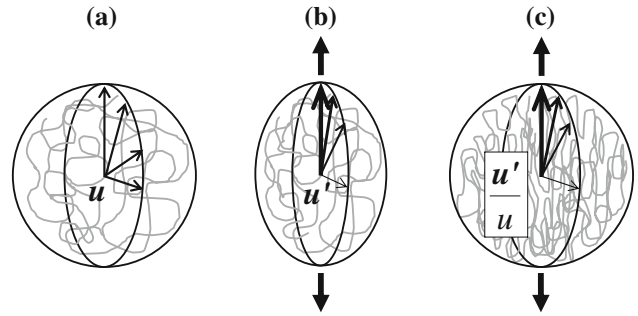


**Fig. 1** Unit vectors (a) in equilibrium, (b) after inception of uniaxial deformation (c) upon saturation of the orientation vector

later developed into a pre-averaged chain stretch term,  $\lambda(t)$ , can be applied to the stress tensor in Eq. 1 to obtain:

$$\sigma = -p\mathbf{I} + \lambda^2(t) \int_{-\infty}^t m(t-t') \mathbf{S}_{DE}^{IA}(t,t') dt' \tag{5}$$

the scalar  $\lambda(t)$  needs to be described by an evolution equation which, as suggested by Pearson et al., can be obtained by assuming the stretch to arise from environment friction (the stretching or convective term) and, at the same time, resisted by a Rouse-like tendency to retract (the retraction or dissipative term) [19, 20]:

$$\frac{d\lambda}{dt} = \left. \frac{d\lambda}{dt} \right|_{\text{Stretching}} + \left. \frac{d\lambda}{dt} \right|_{\text{Retraction}} = \kappa : \bar{\mathbf{S}}\lambda - \frac{1}{\tau_R}(\lambda-1)c(\lambda) \tag{6}$$

Equation 6 in its original form with  $c(\lambda) = 1$  and in combination with Eq. 5 is a convenient first approximation of chain stretch as it can be solved analytically and can predict the experimentally observed overshoots of shear stress and the first normal stress difference that could not be explained by the original DE theory. However, Eqs. 5 and 6 cannot predict strain-hardening when  $\dot{\epsilon}\tau_R < 1$  and more importantly, chain stretch is unbounded according to this description. By accommodating the retraction term in Eq. 6. with a limiting  $c(\lambda)$  function and introducing a material parameter  $\lambda_{max}$ , Ianniruberto and Marrucci [21] and Fang et al. [22] showed that qualitative predictions of the overshoot in nonlinear shear and elongation can be improved significantly. Nonetheless, the pre-averaged chain concept has more important drawback which limits its computational capability: it practically neglects the history of deformation by computing the chain stretch outside of the integral in Eq. 5 [23]. An alternative to the pre-averaged chain stretch concept is based on assuming the tube diameter to represent the mean field of the surrounding chains.

By adding a suitable damping function to the integral in rubber-like liquid theory of Lodge

$$\boldsymbol{\sigma} = -p\mathbf{I} + \int_{-\infty}^t m(t-t')h(I, II)\mathbf{C}^{-1}dt'$$

Wagner [24, 25] has shown that the predictions of elongational and non-linear shear results are remarkably improved. The same concept was applied to obtain a structural model based partly on earlier studies by Marrucci [see e.g., Ref. 26] and introduction of the Molecular Stress Function

$$f = \frac{a_0}{a(t, t')} \tag{7}$$

where  $a_0$  denotes tube diameter before deformation and  $f$  is associated into the original integral in Eq. 1 as:

$$\boldsymbol{\sigma} = -p\mathbf{I} + \int_{-\infty}^t m(t-t')f^2(t, t')\mathbf{S}_{DE}^{IA}(t, t')dt' \tag{8}$$

$f^2$  needs to be calculated by solving a balance equation between two energy arguments: work of the stress tensor and strain energy by decrease in tube diameter [27]. Marrucci et al. [28] have shown that  $f^2$  is a function of the orientational free energy,  $\langle \ln(u') \rangle$ . Wagner et al. showed that this simple, parameter-free presentation can lead to a significant improvement in the quality of predictions at the onset of strain-hardening for HDPE and LDPE melts in uniaxial, equibiaxial, and planar deformations and the shear stress overshoot for non-linear shear deformations [27–29]. However, predictions of the MSF theory for strongly strain-hardening melts such as those of LDPE’s needed a slight modification, as it is well-known that the elongational viscosity curves of highly branched PE’s show a typically sharp increase upon inception of strain-hardening and a higher plateau. The variable  $f^2$  in this case was calculated using an evolution equation of the form:

$$\frac{df^2}{dt} = \frac{\beta f^2}{1 + \frac{\beta-1}{f^4}} \left[ (\boldsymbol{\kappa} : \mathbf{S}) - \frac{1}{f^2 - 1} CR \right] \tag{9}$$

where  $\boldsymbol{\kappa}$  is the velocity gradient tensor and  $\beta$  is a parameter of the MSF theory indicating the number of side chains pressed onto the backbone. As seen in Fig. 2, the macroscopic energy is now consumed by the stretching of backbone in the flow direction and simultaneous compression of side chains, whose quantity is designated by  $\beta$ , on the backbone.  $\beta = 1$  demonstrates the case of a linear chain and  $\beta$  values larger than 1 are related an increase in side chain branching. CR is the term that represents non-linear constraint release and modifies the energy balance of tube deformation so that chain stretch reaches an equilibrium value. This is done by assuming that the orientational part of the strain energy function has

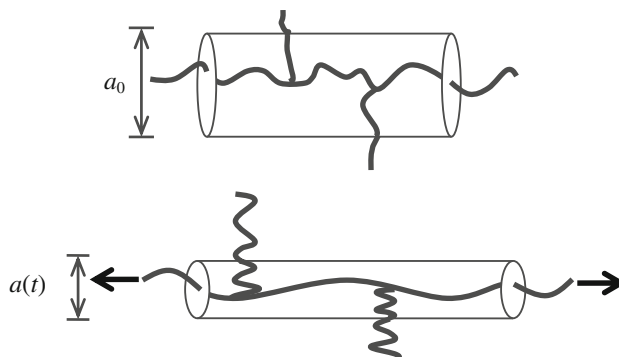


Fig. 2 Tube segment with long-chain branching a before and b after inception of uniaxial deformation

a potential and constraint release is considered to be the consequence of convection mechanisms for both tube orientation and tube-cross section [27]. Hence the constraint release part in Eq. 9 is defined as:

$$CR = \dot{\epsilon} \left[ \frac{f^2 - 1}{f_{max}^2 - 1} \sqrt{S_{11} + \frac{1}{2}S_{33}} \right] \tag{10}$$

where  $S_{11}$  and  $S_{33}$  denote the components of the orientation tensor parallel and perpendicular to stretch direction and  $\dot{\epsilon}$  is the elongation rate.  $f_{max}^2$  is the second parameter of the MSF theory and denotes the maximum tube stretch or the maximum elastic strain energy stored in the molecule. By selecting appropriate values for MSF parameters  $\beta$  and  $f_{max}^2$  and using the final form of Eq. 10 for the case of uniaxial elongation:

$$\frac{\partial f^2}{\partial t} = \dot{\epsilon} \frac{\beta f^2}{1 + \frac{\beta-1}{f^4}} \left[ S_{11} - S_{33} - \frac{f^2 - 1}{f_{max}^2 - 1} \sqrt{S_{11} + \frac{1}{2}S_{33}} \right] \tag{11}$$

it will be possible to predict the elongational viscosities of a large variety of both industrial and model polymer systems. The MSF theory has already been able to give excellent predictions of uniaxial viscosities for LDPE’s with different degrees of branching [30] and model polystyrenes with comb-like structure [31]. The significance of the MSF theory is in its applicability to predict the behavior of both industrial polyolefins with different branching levels and model PS systems with predefined branching structures.

**Predictions for model branched systems**

From now on, Eq. 11 will be used in combination with Eq. 8 to calculate the values of elongational viscosities for all the materials mentioned in this study. The memory function in Eq. 4 will be calculated using the relaxation spectra from Table 1, which is obtained by oscillatory

**Table 1** Relaxation spectra of materials studied in this study

<i>PS-70-3.2G</i>		<i>PS-80-0.6G</i>		<i>FT3200</i>		<i>FA3220</i>	
$g_i$	$\tau_i$	$g_i$	$\tau_i$	$g_i$	$\tau_i$	$g_i$	$\tau_i$
$4.819 \times 10^5$	$2.230 \times 10^{-3}$	$3.533 \times 10^{-2}$	$3.164 \times 10^2$	$2.74 \times 10^5$	$1.60 \times 10^{-4}$	$2.863 \times 10^5$	$1.741 \times 10^{-4}$
$1.375 \times 10^5$	$1.234 \times 10^{-2}$	$5.363 \times 10^0$	$4.725 \times 10^1$	$8.30 \times 10^4$	$1.30 \times 10^{-3}$	$8.955 \times 10^4$	$1.539 \times 10^{-3}$
$8.378 \times 10^4$	$6.811 \times 10^{-2}$	$2.441 \times 10^3$	$7.806 \times 10^0$	$5.30 \times 10^4$	$5.80 \times 10^{-3}$	$5.348 \times 10^5$	$7.048 \times 10^{-3}$
$3.257 \times 10^4$	$3.767 \times 10^{-1}$	$1.816 \times 10^4$	$1.276 \times 10^0$	$3.17 \times 10^4$	$2.57 \times 10^{-3}$	$3.552 \times 10^4$	$3.435 \times 10^{-2}$
$1.177 \times 10^4$	$2.080 \times 10^0$	$4.781 \times 10^4$	$1.983 \times 10^{-1}$	$1.96 \times 10^4$	$1.02 \times 10^{-1}$	$2.056 \times 10^4$	$1.673 \times 10^{-1}$
$2.620 \times 10^3$	$1.149 \times 10^1$	$7.910 \times 10^4$	$2.999 \times 10^{-2}$	$1.18 \times 10^4$	$3.91 \times 10^{-1}$	$1.052 \times 10^4$	$7.893 \times 10^{-1}$
$9.717 \times 10^1$	$6.347 \times 10^1$	$1.316 \times 10^5$	$4.130 \times 10^{-3}$	$6.80 \times 10^3$	$1.46 \times 10^0$	$4.556 \times 10^3$	$3.670 \times 10^0$
$3.310 \times 10^{-3}$	$3.506 \times 10^2$	$4.247 \times 10^5$	$6.100 \times 10^{-4}$	$3.74 \times 10^3$	$5.55 \times 10^0$	$1.440 \times 10^3$	$1.760 \times 10^1$
				$1.72 \times 10^3$	$2.42 \times 10^1$	$3.816 \times 10^2$	$9.247 \times 10^1$
				$7.00 \times 10^2$	$1.29 \times 10^2$		
<i>180HMS</i>		<i>130HMS</i>		<i>SSC23</i>		<i>SSC75</i>	
$g_i$	$\tau_i$	$g_i$	$\tau_i$	$g_i$	$\tau_i$	$g_i$	$\tau_i$
$9.187 \times 10^4$	$8.288 \times 10^{-4}$	$8.781 \times 10^4$	$9.535 \times 10^{-4}$	$3.403 \times 10^5$	$1.620 \times 10^{-4}$	$1.123 \times 10^5$	$1.583 \times 10^{-3}$
$2.652 \times 10^4$	$4.665 \times 10^{-3}$	$2.265 \times 10^4$	$6.210 \times 10^{-3}$	$7.578 \times 10^4$	$3.124 \times 10^{-3}$	$4.171 \times 10^4$	$9.748 \times 10^{-3}$
$1.445 \times 10^4$	$2.023 \times 10^{-2}$	$1.094 \times 10^4$	$2.868 \times 10^{-2}$	$5.463 \times 10^4$	$1.556 \times 10^{-2}$	$1.739 \times 10^4$	$5.089 \times 10^{-2}$
$6.921 \times 10^3$	$8.600 \times 10^{-2}$	$5.477 \times 10^3$	$1.300 \times 10^{-1}$	$2.758 \times 10^4$	$8.974 \times 10^{-2}$	$4.755 \times 10^3$	$2.689 \times 10^{-1}$
$3.014 \times 10^3$	$3.575 \times 10^{-1}$	$2.523 \times 10^3$	$5.917 \times 10^{-1}$	$1.092 \times 10^4$	$4.699 \times 10^{-1}$	$1.122 \times 10^3$	$1.385 \times 10^0$
$1.208 \times 10^3$	$1.465 \times 10^0$	$1.088 \times 10^3$	$2.696 \times 10^0$	$4.310 \times 10^3$	$2.425 \times 10^0$	$1.831 \times 10^2$	$6.792 \times 10^0$
$4.337 \times 10^2$	$5.859 \times 10^0$	$4.460 \times 10^2$	$1.239 \times 10^1$	$1.605 \times 10^3$	$1.201 \times 10^1$	$1.160 \times 10^1$	$3.570 \times 10^1$
$1.311 \times 10^2$	$2.289 \times 10^1$	$1.703 \times 10^2$	$6.465 \times 10^1$	$4.620 \times 10^2$	$5.775 \times 10^1$		
$3.350 \times 10^1$	$9.829 \times 10^1$	$3.223 \times 10^1$	$1.232 \times 10^3$	$8.327 \times 10^1$	$3.038 \times 10^2$		
<i>SSC86</i>				<i>SSC91</i>			
$g_i$	$\tau_i$	$g_i$	$\tau_i$	$g_i$	$\tau_i$	$g_i$	$\tau_i$
$1.331 \times 10^5$		$1.105 \times 10^{-3}$		$1.543 \times 10^5$			$9.125 \times 10^{-4}$
$3.598 \times 10^4$		$9.055 \times 10^{-3}$		$4.666 \times 10^4$			$6.387 \times 10^{-3}$
$1.099 \times 10^4$		$5.161 \times 10^{-2}$		$1.836 \times 10^4$			$2.985 \times 10^{-2}$
$2.401 \times 10^3$		$2.956 \times 10^{-1}$		$5.212 \times 10^3$			$1.360 \times 10^{-1}$
$3.516 \times 10^2$		$1.642 \times 10^0$		$1.223 \times 10^3$			$6.138 \times 10^{-1}$
$2.224 \times 10^1$		$9.201 \times 10^0$		$2.194 \times 10^2$			$2.645 \times 10^0$
				$1.864 \times 10^1$			$1.165 \times 10^1$

shear measurements. Details of the measurement method for model polystyrenes are given in Refs. [18, 31]. In Fig. 3 predictions of the DE and MSF with different parameters are shown for a model PS, mentioned in an earlier study by Wagner et al. [31]. These materials can be produced in a two-step process giving side chains with a predefined length that are grafted in a radical polymerization process onto the main backbone [18]. The comb polystyrenes which are schematically shown in Fig. 3 were then used as models with well-defined branching to examine the accuracy of the MSF theory in giving a simple, yet useful picture of the relative number of side chains. Having the average number of side chains grafted to the backbone,  $\alpha$ ,

and the number average molecular weights of backbone,  $M_{n, BB}$ , and side chains,  $M_{n, SC}$ ,  $\beta$  can be given by:

$$\beta = 1 + \alpha \frac{M_{n, SC}}{M_{n, BB}} \quad (12)$$

Using the  $\beta$  values calculated by Eq. 12, the MSF model can successfully predict the elongational behavior of model branched polystyrenes with  $\beta$  values ranging from 1 to 2. PS samples with side chains shorter than the entanglement length essentially behave as linear polymers, which is associated with a value of  $\beta = 1$  according to the MSF theory. The results from elongation tests for two of the

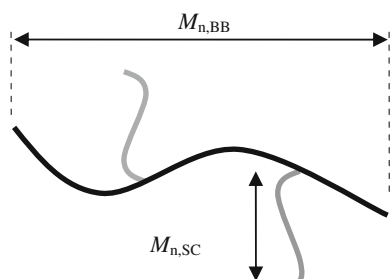


**Fig. 3** Schematic presentation of a model comb PS with radically grafted side chains.  $M_{n,BB}$  and  $M_{n,SC}$  are the number average molecular weights of backbone and branches, respectively. If in the grafting process an average of  $\alpha$  side chains have been grafted to the backbone, then the value of MSF parameter  $\beta$  can be calculated by  $\beta = 1 + \alpha \frac{M_{n,SC}}{M_{n,BB}}$

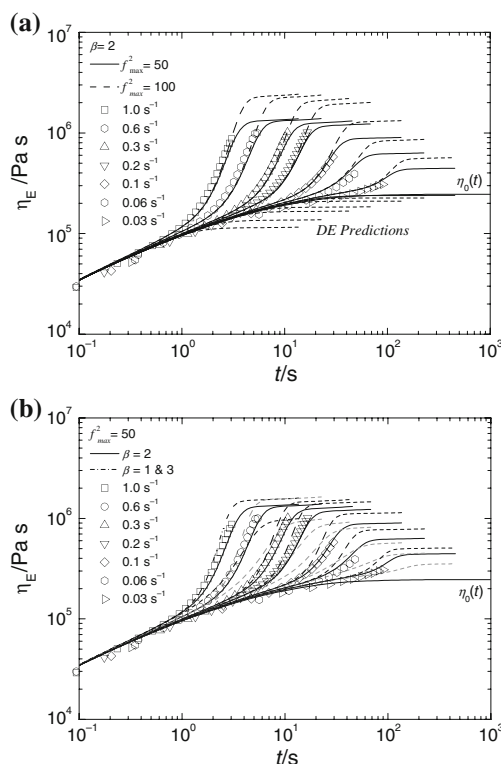


**Fig. 4** Elongational viscosities of a comb PS with 3.2 side chains with  $M_{n,SC} = 22,000$  g/mol grafted to a backbone with  $M_{n,BB} = 70,000$  g/mol with MSF parameters **a**  $\beta = 2$  and  $f_{max}^2 = 50$  and 100 compared to DE predictions. **b**  $f_{max}^2 = 50$  and  $\beta = 1, 2$  and 3 (shown in *dotted gray*, *full black* and *dotted black* lines, respectively). The branching parameter  $\beta = 2$  is obtained using Eq. 12 knowing the reaction parameters [Experimental data from Ref. 31]

model polystyrenes mentioned in [31] are compared with MSF predictions in Figs. 4 and 5. In Fig. 4, the elongational data of a PS with 3.2 side chains ( $\alpha = 3.2$ ) which have a number average molar mass of  $M_{n,SC} = 22,000$  g/mol and are grafted to a backbone with  $M_{n,BB} = 70,000$  g/mol are shown. Predictions of the MSF theory for two different  $f_{max}^2$

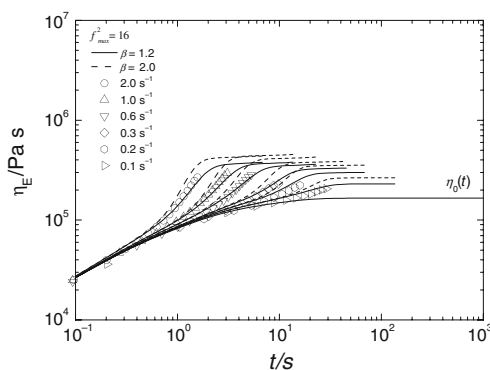


**Fig. 5** Elongational viscosities of a comb PS with  $\alpha = 0.6$ ,  $M_{n,SC} = 22,000$  g/mol and  $M_{n,BB} = 70,000$  g/mol which suggest that a branching parameter  $\beta = 1.2$  is suitable for the MSF predictions. For comparison, predictions for  $\beta = 2$  are shown which obviously overestimate the elongational viscosities [Experimental data from Ref. 31]

values are compared to those of DE theory and experimental results. The DE theory clearly underestimates the elongational viscosities due to lack of chain stretch in the model (shown in Fig. 4a as dotted lines lying below the LVE curve). To simulate the elongation results using the MSF theory, a value of  $\beta = 2$  was calculated based on the characteristics from the synthesis, and it can be seen that the right choice of  $f_{max}^2 = 50$  leads to very good predictions of the plateau of elongational viscosities for all elongation rates. In Fig. 4b the simulation results are shown for the same model PS, but again three different  $\beta$  values (1, 2, and 3) have been selected for comparison. As can be seen, this parameter describes the onset of strain hardening in elongation and slope of elongational viscosities before reaching the plateau, and only  $\beta = 2$  gives correct predictions for elongational viscosities (shown in Fig. 4b as full black lines). In Fig. 5, the elongational viscosities of another model PS from Ref. [31] with  $\alpha = 0.6$ ,  $M_{n,SC} = 22,000$  g/mol and  $M_{n,BB} = 70,000$  g/mol are shown. Using Eq. 12, a branching parameter of  $\beta = 1.2$  can be obtained which seems to perfectly predict the onset of strain-hardening. Dotted lines in Fig. 5 show MSF predictions for  $\beta = 2$ , which has been selected for comparison.

### Predictions for industrial polyolefins

Oscillatory shear for the polyolefins was performed at 180 °C on an MCR300 rotational rheometer from Anton Paar, with plate–plate geometry and a gap of 1.3 mm. Elongational rheology was performed at 180 °C with a SER tool attached to an MCR501 rotational rheometer from Anton Paar.

The excellent agreement between experimental results and theoretical predictions for model polystyrenes

mentioned in the previous section prove that the MSF theory can use only two parameters, whereas at least one of the parameters,  $\beta$ , can be obtained by knowledge of the structure. Unfortunately, there is still no equation similar to Eq. 12 for industrial polyolefins, namely branched PE and PP, where the production method often guarantees no quantitative knowledge of branching structure and even molecular weight distribution. In addition, the post-reactor processes are known to contribute to a high level of disorder in molecular architecture [32, 33]. In this part, we will show the predictions of the MSF theory for a series of four commercial branched PE and PP grades from Borealis and four PP's from bench-scale polymerization. However, we need to emphasize that the MSF parameters, in lack of a more suitable technique to characterize branching in a fast and consistent way, only provide a method for comparing materials of the same group.

The first group of materials consists of two branched LDPE grades, FT3200 and FA3220 and two branched high-melt strength PP grades, WB180HMS and WB130HMS. It is known that WB130HMS and FA3220 have more branching than WB180HMS and FT3200, respectively. In the case of PE's in the current study, FA3220 is from an autoclave reactor whereas FT3200 is from a tubular one. Tubular reactors are known to produce more regular branching structure compared to the autoclave reactors, which produce longer side chains and hyperbranching by increasing the availability of radicals. Wagner et al. [30] have shown that the elongational rheology of a typical tubular PE can be described by  $\beta = 2$  whereas an autoclave PE has  $\beta$  values between 3 and 4. Further analysis of blends of LLDPE with an autoclave LDPE using the MSF theory revealed in a later study that the elongational behavior of blends, even in the linear range, is highly dependent on the LDPE, at fractions as small as 5% [34]. In Fig. 6 predictions of the MSF theory for elongational rheology of tubular (FT3200) and autoclave (FA3220) LDPE's are shown. The relative branching content can be recognized by a branching parameter  $\beta$  which is larger for the autoclave LDPE ( $\beta = 1.5$ ) compared to the tubular LDPE ( $\beta = 1.3$ ). The difference between  $\beta = 1.3$  and  $\beta = 1.5$  in this case is essentially representative of the structural differences between FA3220 and FT3200, as Wagner et al. [31] have shown for model PS with well-defined branching structure. These  $\beta$  values are smaller compared to those obtained by Wagner et al. [30], but are consistent with the fact that autoclave LDPE's normally have higher branching degrees than tubular ones. The plateaus of the elongational viscosities at different elongation rates can be consistently predicted by a single  $f_{\max}^2$  parameter in the case of the tubular LDPE, whereas  $f_{\max}^2$  has different values in the case of autoclave LDPE. We

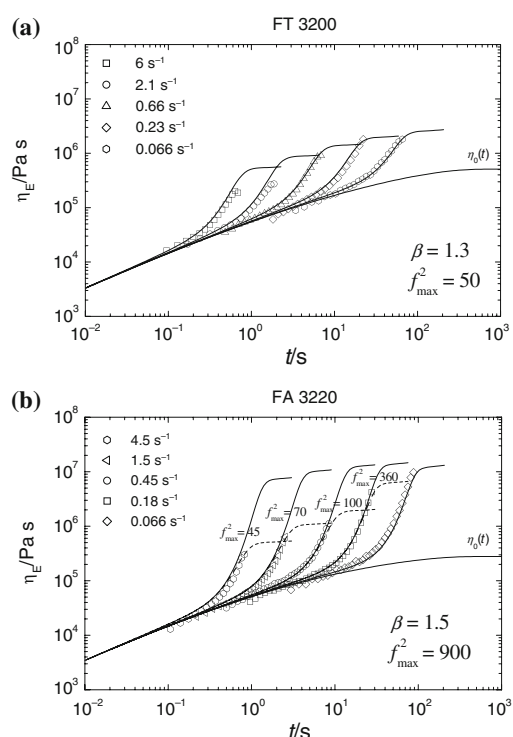


**Fig. 6** Elongational viscosities of **a** tubular and **b** autoclave LDPE's. Parameter  $\beta$  can consistently describe the branching content of the two essentially different branching structures. In the case of autoclave LDPE the plateaus of the elongational viscosity show a dependence on elongation rate

speculate this to be a result of the irregular branching structure of FA3220 in comparison to FT3200.

Elongational rheology of branched PP's has only recently attracted attention due to its increasing industrial applications in foaming and film production [35–39]. For branched PP's produced by gamma irradiation, Wagner et al. [40] have already shown that the MSF theory can predict the elongational behavior with excellent precision. Predictions of the MSF theory for two high melt strength polypropylenes, produced by post-reactor modification [39] of a linear PP are shown in Fig. 7. WB180HMS, a material used for stretched film applications, is known to have a lower melt strength in comparison to WB130HMS which is used for foaming [8, 9]. The structural difference between both materials is demonstrated very well in the difference in MSF parameters. Elongational viscosities of WB180HMS can be predicted with  $\beta = 1.3$  and  $f_{\max}^2 = 80$  whereas WB130HMS shows a stronger strain hardening that can be predicted with  $\beta = 2$  and  $f_{\max}^2 = 250$ . Also in this case, the MSF parameters can be used as material-specific values to compare the amount of branching and the intensity of strain-hardening for two commercial products.

Finally, the elongational viscosities of a series of PP's produced in a bulk process with zirconocene catalysts are

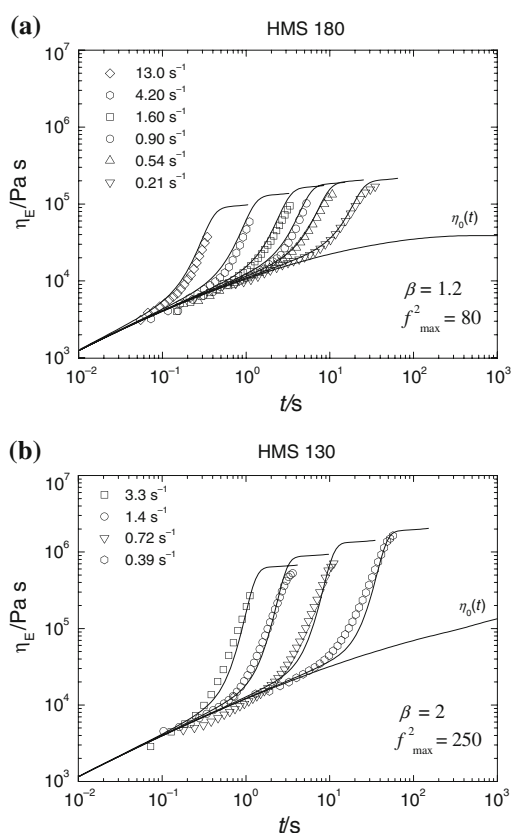


**Fig. 7** Elongational viscosities of two High Melt Strength (HMS) PP grades **a** WB180HMS and **b** WB130HMS, with different degrees of branching, implied by two different  $\beta$  values:  $\beta = 1.2$  for WB180HMS and  $\beta = 2$  for WB130HMS

**Fig. 8** Elongational rheology of metallocene polypropylenes.

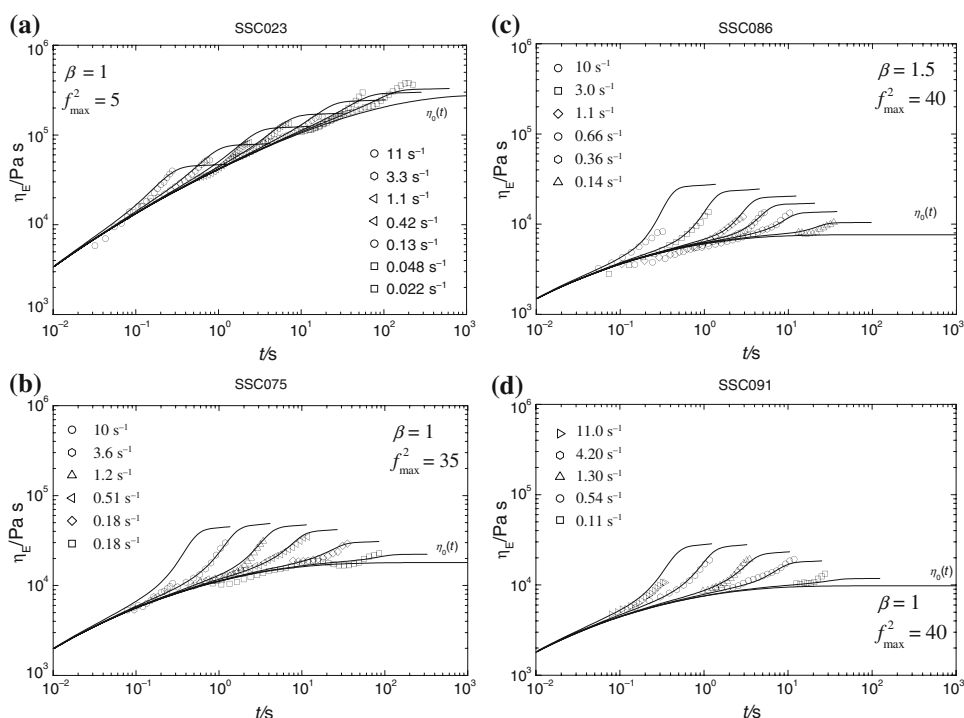
**a** Linear PP with MFR < 1 and 0.5% C2 as comonomer.

**b** Branched PP with 0.5% C2 as comonomer and MFR  $\sim 4.6$ .

**c** Branched PP homopolymer with MFR  $\sim 10.7$ .

**d** Branched PP with 0.5% C2 as comonomer and MFR  $\sim 8.6$ .

The higher  $\beta$  value of homo-PP in **c** suggests that it has a comparably higher branching in its structure



shown in Fig. 8. Detailed description of this new class of PP's has been published recently [13] with a quantitative assessment of branching based on elongational viscosity measurements [7, 10, 12].

All four materials were produced under the same temperature and pressure conditions but differed in their  $M_w$  and comonomer content. SSC23 is a linear, high  $M_w$  polypropylene. SSC23, SSC75, and SSC91 are polymerized with 0.5% C2 as comonomer, whereas SSC86 is a homopolymer. These materials can be sorted in terms of their  $M_w$  as follows:

$$SSC23 > SSC75 > SSC91 > SSC86$$

Despite its essentially linear structure, SSC23 has a weak yet appreciable strain-hardening which can be characterized with  $\beta = 1$  and  $f_{\max}^2 = 5$ . This can be attributed to the possible existence of a high  $M_w$  shoulder in the distribution that cannot be distinguished by other analytical methods. The MSF theory has already shown to be capable of detecting very small amounts of a very high  $M_w$  fraction in model PS blends [41]. Strain-hardening in the copolymers SSC75 and SSC91 is stronger and can be described by the same  $\beta$  ( $=1$ ) but a larger  $f_{\max}^2$  (35 for SSC75 and 40 for SSC91). Finally, the homopolymer SSC86 shows a relatively stronger strain-hardening and a larger branching parameter  $\beta = 1.5$ , compared to the other three SSC-PP's, being the only PP in this group to have  $\beta > 1$ . The value of  $\beta = 1$  for the other three PP's in this group might not necessarily show the existence of long

chain branching in the sense of the MSF theory. However, since the structure of this new class of strain-hardening PP's is not thoroughly studied, the authors can speculate that it might be related to the existence of a very small long-chain-branched phase that can lead to the weak strain-hardening seen in the elongation curves.

## Conclusions

The capability of constitutive equations in predicting the non-linear elongational behavior of industrial polymers has always been limited by the quality of experimental results and availability of a reliable theoretical method to interpret those results. In this respect, the molecular stress function theory provides a consistent framework to analyze the results from non-linear elongational measurements and have a quantitative basis for comparison among materials with different branching structures. We have showed in the current study that the MSF theory can excellently predict the elongational behavior of model branched PS materials using only one structure-based parameter that can be calculated using the real picture of the branching, obtained from reaction conditions. At the same time, the MSF theory can give very good predictions for the elongational behavior of branched PE's and PP's with the possibility to compare the intensity of strain-hardening and have a solid judgment about the structure. This finding is remarkable as it proves that the MSF theory can provide precise information on the amount of branching for a wide variety of industrial polyolefins. In this respect, it addresses one of the most critical challenges in the development of metallocene PP's, which is to find a correlation between their processing behavior and their structure.

## References

- Field GJ, Micic P, Bhattacharya SN. Melt strength and film bubble instability of LLDPE/LDPE blends. *Polym Int*. 1999;48:461–6.
- Lohse DJ, Milner ST, Fetters LJ, Xenidou M, Hadjichristidis N, Mendelson RA, et al. Well-defined, model long-chain branched polyethylene. 2. Melt rheological behavior. *Macromolecules*. 2002;35:3066–75.
- Hussein IA. Influence of composition distribution and branch content on the miscibility of m-LLDPE and HDPE blends: rheological investigation. *Macromolecules*. 2003;36:2024–31.
- Stephens CH, Hiltner A, Baer E. Phase behavior of partially miscible blends of linear and branched polyethylenes. *Macromolecules*. 2003;36:2733–41.
- Mieda N, Yamaguchi M. Anomalous rheological response for binary blends of linear polyethylene and long chain-branched polyethylene. *Adv Polym Tech*. 2008;26:173–81.
- Liu C, Wang J, He J. Rheological and thermal properties of m-LLDPE blends with m-HDPE and LDPE. *Polymer*. 2002;43:3811–8.
- Stadlbauer M, Ernst E. Polypropylene foam. European Patent 2008; EP1900764A1.
- Rätzsch M, Hesse A, Bucka H, Reichelt N, Panzer U, Bühler K. Polyolefinschaumstoffe hoher Wärmeformbeständigkeit. European Patent 1998; EP0879844A1.
- Stadlbauer M, Kirchberger M. A polyolefin foam. European Patent 2007; EP1754744A1.
- Stadlbauer M, Kirchberger M, Ernst E. Extrusion coated substrate. European Patent 2008; EP1967547A1.
- Hesse A, Panzer U, Paulik C, Wolfsberger A, Kirchberger M, Niedersüss P. Polyolefinfolien und Polyolefinbeschichtungen von Substraten. European Patent 1999; EP0947551A1.
- Stadlbauer M, Ernst E, Niedersüss P. Blown film of polypropylene. European Patent 2008; EP1903070A1.
- Ernst E, Stadlbauer M. Multi-branched polypropylene. European Patent EP 2007; 1847555.
- de Gennes PG. Reptation of polymer chains in presence of fixed obstacles. *J Chem Phys*. 1971;55:572–9.
- Doi M, Edwards SF. *Theory of polymer dynamics*. Oxford: Oxford University Press; 1986.
- Tsenoglou C. Molecular weight polydispersity effects on the viscoelasticity of entangled linear polymers. *Macromolecules*. 1991;24:1762–7.
- van Ruymbeke E, Keunings R, Stéphenne V, Hagenaaers A, Bailly C. Evaluation of reptation models for predicting the linear viscoelastic properties of linear entangled polymers. *Macromolecules*. 2002;35:2689–99.
- Hepperle J, Münstedt H, Haug PK, Eisenbach D. Rheological properties of branched polystyrenes: linear viscoelastic behavior. *Rheol Acta*. 2005;45:151–63.
- Urakawa O, Takahashi M, Masuda T, Golshan Ebrahimi N. Damping functions and chain relaxation in uniaxial and biaxial elongation: comparison with the Doi-Edwards theory. *Macromolecules*. 1995;28:7196–201.
- Pearson DS, Kiss AD, Fetters LJ, Doi M. Flow-induced birefringence of concentrated polyisoprene solutions. *J Rheol*. 1989;33:517–35.
- Ianniruberto G, Marrucci G. A simple constitutive equation for entangled polymers with chain stretch. *J Rheol*. 2001;45:1305–18.
- Fang G, Kröger M, Öttinger HC. A thermodynamically admissible reptation model for fast flows of entangled polymers. II. Model predictions for shear and extensional flow. *J Rheol*. 2000;44:1293–317.
- Mead DW, Larson RG, Doi M. A molecular theory for fast flows of entangled polymers. *Macromolecules*. 1998;31:7895–914.
- Wagner MH, Stephenson SE. The irreversibility assumption of network disentanglement in flowing polymer melts and its effects on elastic recoil predictions. *J Rheol*. 1979;23:489–504.
- Wagner MH. The nonlinear strain measure of polyisobutylene melt in general biaxial flow and its comparison to the Doi-Edwards model. *Rheol Acta*. 1990;29:594–603.
- Marrucci G, de Cindio B. The stress relaxation of molten PMMA. *Rheol Acta*. 1980;19:68–75.
- Wagner MH, Rubio P, Bastian H. The molecular stress function model for polydisperse and polymer melts with dissipative convective constraint release. *J Rheol*. 2001;45:1387–412.
- Marrucci G, Grizzutti N. The free energy function of the Doi-Edwards theory: analysis of instabilities in stress relaxation. *J Rheol*. 1983;27:433–50.
- Wagner MH, Bastian H, Hachmann P, Meissner J, Kurzbeck S, Languche F. The strain hardening behaviour of linear and long-chain-branched polyolefin melts. *Rheol Acta*. 2000;39:97–109.
- Wagner MH, Yamaguchi M, Takahashi M. Quantitative assessment of strain hardening of LDPE melts by MSF model. *J Rheol*. 2003;47:779–93.



31. Wagner MH, Hepperle J, Münstedt H. Relating molecular structure of model branched polystyrene melts to strain-hardening by molecular stress function theory. *J Rheol*. 2004;48:489–503.
32. Ohnishi R, Fujimura T, Tsunori R, Sugita Y. A new method for producing high melt strength poly(propylene) with reactive extrusion. *Macromol Mater Eng*. 2005;290:1127–234.
33. Auhl D, Stange J, Münstedt H, Krause B, Voigt D, Lederer A, et al. Long-chain branched polypropylenes by electron beam irradiation and their properties. *Macromolecules*. 2004;37:9465–72.
34. Wagner MH, Kheirandish S, Yamaguchi M. Quantitative analysis of melt elongational behavior of LDPE/LLDPE blends. *Rheol Acta*. 2005;44:198–218.
35. Münstedt H, Kurzbeck S, Stange J. Importance of elongational properties of polymer melts for film blowing and thermoforming. 2006;46:1190–5.
36. Sadeghi F, Ajji A, Carreau PJ. Analysis of row nucleated lamellar morphology of polypropylene obtained from the cast film process: effect of melt and process conditions. *Polym Eng Sci*. 2007;47:1170–8.
37. Sadeghi F, Ajji A, Carreau PJ. Microporous membranes obtained from polypropylene blends superior with permeability properties. *J Polym Sci B Polym Phys*. 2008;46:148–57.
38. Stadler FJ, Nishioka A, Stange J, Koyama K, Münstedt H. Comparison of the elongational behavior of various polyolefins in uniaxial and equibiaxial flows. *Rheol Acta*. 2007;46:1003–12.
39. Rätzsch M, Bucka H, Hesse A, Panzer U, Reichelt N. Strukturisomere Poly(alkylethylene). European Patent 1997; EP0787750A2.
40. Wagner MH, Kheirandish S, Stange J, Münstedt H. Modeling elongational viscosity of blends of linear and long-chain branched polypropylenes. 2006;46:211–22.
41. Wagner MH, Kheirandish S, Koyama K, Nishioka A, Minegishi A, Takahashi T. Modeling strain hardening of polydisperse polystyrene melts by molecular stress function theory. *Rheol Acta*. 2005;44:235–43.